Infrared Spectra of Antimony and Bismuth Hydrides in Solid Matrixes

Xuefeng Wang, Philip F. Souter, and Lester Andrews*

Department of Chemistry, University of Virginia, P.O. Box 400319, Charlottesville, Virginia 22904-4319

Received: February 13, 2003; In Final Form: March 26, 2003

Laser-ablated Sb and Bi atoms react with hydrogen during condensation in excess hydrogen, neon, and argon to form the SbH and BiH diatomic molecules. In addition the new Group 15 MH_2 dihydride radicals and the MH_3 trihydrides are observed for Sb and Bi metals. Although BiH_3 is of limited stability in the gas phase, BiH_3 is formed by further H atom reactions with BiH_2 in solid hydrogen and neon. No evidence is found for the thermochemically unstable BiH_5 molecule.

Introduction

Bismuthine is of interest as the heaviest member of the ammonia family of molecules, in part, because of limited stability and relativistic contributions to bonding and structure. An important reference book states that "bismuthine is too unstable to be of any importance".[1] However, BiH_3 was prepared in 1961.[2] Recently this demanding synthesis was repeated, and the BiH_3 product was verified during its 10−30 min lifetime by high-resolution spectroscopy.[3] Several electronic structure calculations have been performed on BiH_3 to explore relativistic effects on the structure, inversion barrier, and vibrational frequencies.[3−8] In addition, BiH_5 has been computed by two research groups; the average bond energy is less than found for BiH_3,[5] and BiH_5 is less stable than $BiH_3 + H_2$.[9]

The monohydride BiH has been investigated in the gas phase by diode laser spectroscopy, and accurate bond length and vibrational frequency measurements have been made.[10−13] A number of electronic structure calculations have been performed on BiH with spin−orbit splitting and relativistic effects a major part of the motivation.[5,7,14−19] There are no experimental data on the BiH_2 radical, but its ionization energy has been calculated.[16] Finally, sixth-row p-block metal hydride dimers have been explored by theory, and a trans structure has been proposed for Bi_2H_2.[20]

Laser-ablated metal atom reactions with pure hydrogen have been employed in our laboratory to synthesize such reactive hydrides as $(H_2)CrH_2$ and PbH_4,[21,22] and by other research groups.[23,24] Therefore we use this method for BiH, BiH_2, BiH_3, and Bi_2H_2 investigation and take advantage of straightforward deuterium substitution. Similar experiments were done with antimony for comparison of heavy Group 15 hydrides.

Experimental and Computational Methods

The experimental method for laser-ablation and matrix-isolation has been described in detail previously.[25,26] Briefly, the Nd:YAG laser fundamental (1064 nm, 10 Hz repetition rate with 10 ns pulse width) was focused to irradiate rotating metal targets (Johnson-Matthey). Typically, low laser power (3−5 mJ/pulse) was used to ablate metal atoms into condensing hydrogen, neon/H_2, or argon/H_2 on a 3.5 K CsI window. Normal hydrogen, deuterium (Matheson), HD (Cambridge Isotopic Laboratories), and $H_2 + D_2$ mixtures were used in different experiments. Infrared spectra were recorded at 0.5 cm^{-1} resolution on a Nicolet 750 spectrometer with 0.1 cm^{-1} accuracy using a mercury cadmium telluride detector down to 400 cm^{-1}. Matrix samples were annealed at different temperatures, and selected samples were subjected to photolysis using glass filters and a medium-pressure mercury lamp ($\lambda > 240$ nm) with the globe removed.

Density functional theory (DFT) calculations were performed to help identify small reaction products using the GAUSSIAN 98 program.[27] Two generalized gradient approximations consisting of Becke's exchange and Perdew-Wang's correlation (BPW91) functionals[28] and the hybrid Hartree−Fock B3LYP functional[29] were chosen. The 6-311++G** basis set was used for hydrogen,[30] and the SDD effective core potential and basis were used for Bi and Sb.[31]

Results

Laser-ablated Bi and Sb atoms were reacted with pure hydrogen, Ne/H_2, and Ar/H_2 samples, and density functional calculations were done for potential product molecules.

Bismuth. Figure 1 illustrates the 1760−1580 cm^{-1} region of the spectrum of laser-ablated Bi co-deposited with pure hydrogen. A sharp, strong 1867.6 cm^{-1} band (not shown) increases relative to the other absorptions with increasing laser energy, and it will be assigned to a Bi_x cluster vibronic transition in a later report. The next strongest feature on deposition is the 1622.7, 1630.0, 1633.3 cm^{-1} band group (labeled BiH), followed by 1692.7 cm^{-1}, 1699.1 cm^{-1} (labeled BiH_2), and a weak 1726.2 cm^{-1} band (labeled BiH_3). Annealing to 6.1 K changed relative intensities in the BiH group favoring the sharp 1633.3 cm^{-1} band (Figure 1b). Irradiation at $\lambda > 470$ nm had little effect on the BiH group, and increased the BiH_2 group (not shown). Similar $\lambda > 380$ nm photolysis altered relative intensities in the BiH group and increased the BiH_3 band (Figure 1c), and $\lambda > 290$ nm photolysis continued this trend. Irradiation at $\lambda > 240$ nm increased the two broader members of the BiH group, completed destruction of the intervening bands, markedly increased the BiH_2 group, and destroyed the weak BiH_3 band (Figure 1d). A subsequent 6.6 K annealing restored the sharp 1633.3 cm^{-1} BiH band at the expense of the broader bands, restored the BiH_2 set, and restored some of the BiH_3 band (Figure 1e). Another experiment gave similar results.

A marked simplification is found for Bi in pure D_2. The strongest feature is 1163.4 cm^{-1} (labeled BiD) with weak 1218.4

* Corresponding author. E-mail: lsa@virginia.edu

10.1021/jp034379y CCC: $25.00
Published on Web 04/29/2003

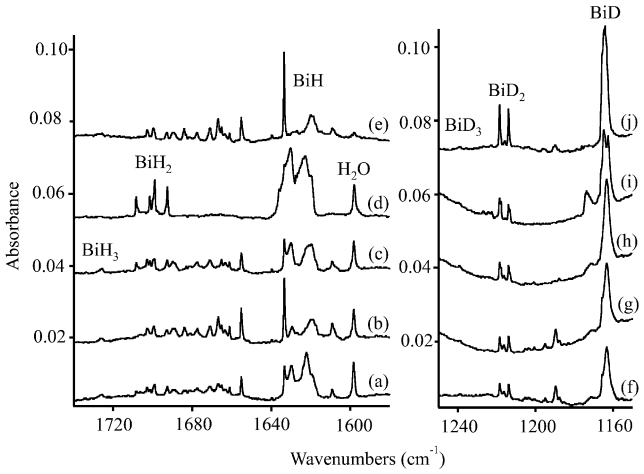

Figure 1. Infrared spectra in the 1740−1580 cm^{-1} and 1250−1150 cm^{-1} regions for laser-ablated Bi atoms co-deposited with normal H_2 and D_2 at 3.5 K. (a) Bi and 60 STPcc of H_2 condensed at 3.5 K, (b) after annealing to 6.1 K, (c) after $\lambda > 380$ nm photolysis, (d) after $\lambda > 240$ nm photolysis, (e) after annealing to 6.6 K, (f) Bi and 60 STPcc of D_2 condensed at 3.5 K, (g) after annealing to 7.2 K, (h) after $\lambda > 290$ nm photolysis, (i) after $\lambda > 240$ nm photolysis, and (j) after annealing to 8.5 K.

TABLE 1: Infrared Absorptions (cm^{-1}) Observed from Co-deposition of Laser-Ablated Bi Atoms and with Ne/H_2, Pure H_2, and Ar/H_2 at 3.5 K

Ne/H_2	Ne/D_2	H_2	D_2	Ar/H_2	Ar/D_2	ident.
2439.4	2438	2438.5	-	2468.8	2469	Bi_x
2157.0	2156	2156.8	2151.4	2185.7	2186	Bi_x
1867.0	1866.4	1867.6	1866.1	1894.3	1894.5	Bi_x
1733.6	1243.4	1726.2	1239.0			BiH_3
		1708.4		1690.9	1213.1	BiH_2 site
		1701.5		1684.0	1208.3	BiH_2 site
1704.9	1223.0	1699.1	1218.4	1693.2	1214.4	BiH_2, ν_3 (b_2)
1698.0	1218.5	1692.7	1214.4	1686.4	1209.5	BiH_2, ν_1 (a_1)
		1670.9		1672.4	1195.4	Bi_xH_y
		1666.9		1662.0		Bi_xH_y
		1661.2				Bi_xH_y
1661.4	1191.0	1655.1	1189.7			Bi_xH_y
		1633.3				BiH site
		1630.0	1165.0			BiH site
1635.9	1171.9	1622.7	1163.4	1621.9	1161.6	BiH
				1612.3	1156.7	Bi_xH_y
		1609.1		1609.8	1154.3	Bi_xH_y
1596.4	1596.4	1598.3	1597.3	1590.0	1590.0	H_2O

cm^{-1}, 1214.4 cm^{-1} (BiD_2), and 1239.0 cm^{-1} (BiD_3) bands, which are shown in the lower region of Figure 1. The Bi_x band at 1866.1 cm^{-1} is substantially weaker. Ultraviolet photolysis had a similar effect on the band groups: BiD and BiD_2 increased (Figure 1h,i). However, annealing to 8.5 K increased BiD and BiD_2 even more (Figure 1j). Subsequent $\lambda > 240$ nm irradiation and 8.8 K annealing reproduced the above spectra. The product absorptions are listed in Table 1.

Experiments were performed with 50/50 and 30/70 mixtures of H_2 and D_2, and spectra in both regions are shown in Figure 2. Strong absorptions at 1623.3 cm^{-1} (BiH) and 1163.2 cm^{-1} (BiD) are slightly different from those of pure hydrogen and deuterium matrix samples. Sharp triplet bands were observed for the dihydrides and slightly shifted 1726.0 and 1238.5 cm^{-1} peaks were observed for the trihydrides. An experiment with pure HD is shown at the top of Figure 2; the BiH (1628.8, 1627.1, 1624.0 cm^{-1}) and BiD (1167.1, 1166.1, 1164.0 cm^{-1}) bands are split, major 1696.2 and 1216.4 cm^{-1} bands acquire weaker sidebands on photolysis and annealing, and weak new bands are found at 1727.7 and 1239.7 cm^{-1}.

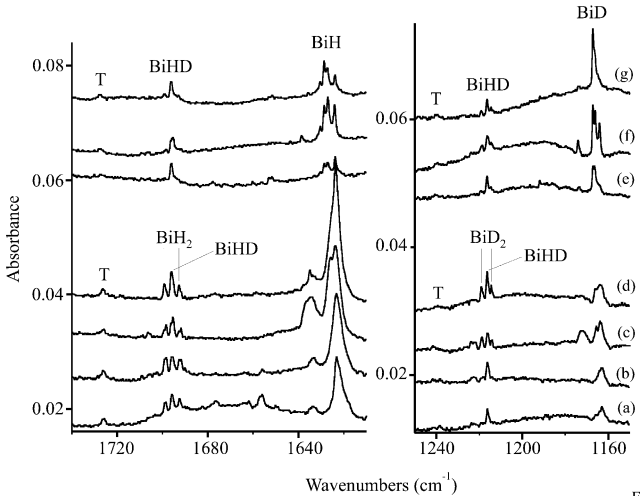

Figure 2. Infrared spectra in the 1740−1610 cm^{-1} and 1250−1150 cm^{-1} regions for laser-ablated Bi atoms co-deposited with mixed isotopic hydrogen at 3.5 K. (a) Bi and 50% H_2 + 50% D_2, (b) after $\lambda > 380$ nm photolysis, (c) after $\lambda > 240$ nm photolysis, (d) after annealing to 6.6 K, (e) Bi and pure HD, (f) after $\lambda > 290$ nm photolysis, and (g) after annealing to 7.1 K. The label T denotes BiH_xD_y ($x + y = 3$).

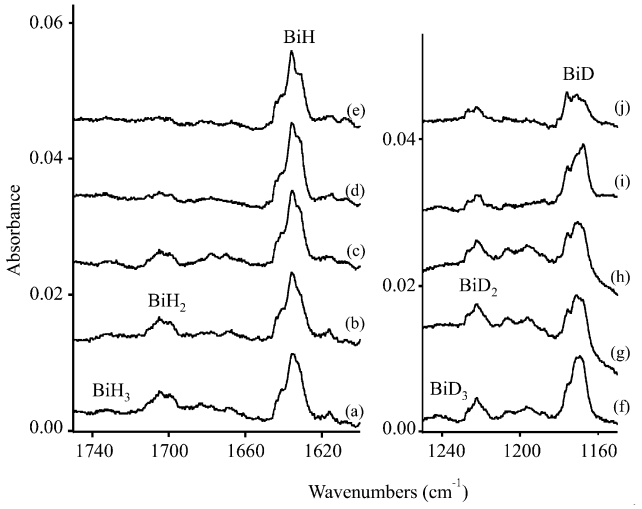

Figure 3. Infrared spectra in the 1740−1610 cm^{-1} and 1250−1150 cm^{-1} regions for laser-ablated Bi atoms co-deposited with Ne/H_2 and Ne/D_2 at 3.5 K. (a) Bi and 10% H_2 in neon, (b) after annealing to 6.2 K, (c) after $\lambda > 380$ nm photolysis, (d) after $\lambda > 290$ nm photolysis, (e) after annealing to 6.5 K, (f) Bi and 10% D_2 in neon, (g) after annealing to 6.1 K, (h) after $\lambda > 380$ nm photolysis, (i) after $\lambda > 240$ nm photolysis, and (j) after annealing to 6.6 K.

Both H_2 and D_2 reactions with Bi in excess neon are illustrated in Figure 3. The major features are 1635.9 cm^{-1} (BiH) and 1171.9 cm^{-1} (BiD), minor absorptions are 1704.9 (BiH_2) and 1223.0 cm^{-1} (BiD_2), and weak new bands are 1733.6 (BiH_3) and 1243.4 cm^{-1} (BiD_3).

The argon matrix spectra of Bi and H_2 reaction products are shown in Figure 4a. The major peak at 1621.9 cm^{-1} (BiH) increases on annealing as do weaker 1693.2, 1686.4 cm^{-1} features with still weaker 1690.9, 1684.0 cm^{-1} satellites (BiH_2), and the Bi_x cluster absorption at 1894.3 cm^{-1}. The corresponding D_2 spectra are compared in Figure 4, which reveals a strong 1161.6 cm^{-1} absorption (BiD) and weaker 1214.4, 1209.5 cm^{-1} bands (BiD_2). The $H_2 + D_2$ experiment gave the same product absorptions. Similar investigations with HD yielded the same strong bands and sharp weaker intermediate features at 1690.0 and 1211.3 cm^{-1}, as illustrated at the top of Figure 4.

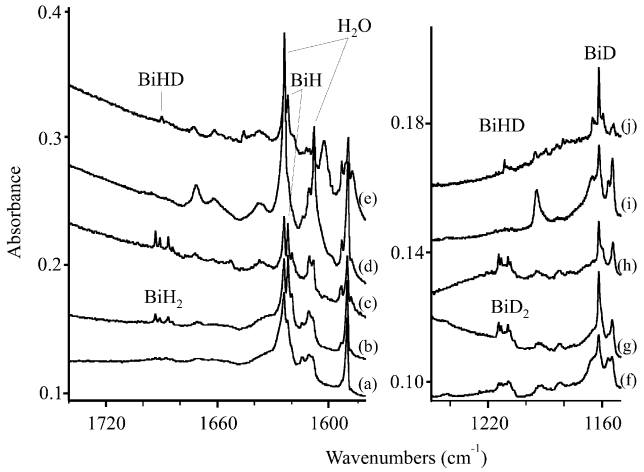

Figure 4. Infrared spectra in the 1740−1580 cm^{-1} and 1250−1150 cm^{-1} regions for laser-ablated Bi atoms co-deposited with H_2, D_2, and HD in excess argon at 3.5 K. (a) Bi and 10% H_2 in argon, (b) after annealing to 17 K, (c) after annealing to 25 K, (d) Bi and 10% HD in argon, (e) after photolysis and annealing to 35 K, (f) Bi and 10% D_2 in argon, (g) after annealing to 19 K, (h) after annealing to 25 K, (i) Bi and 10% HD in argon, (j) after photolysis and annealing to 35 K.

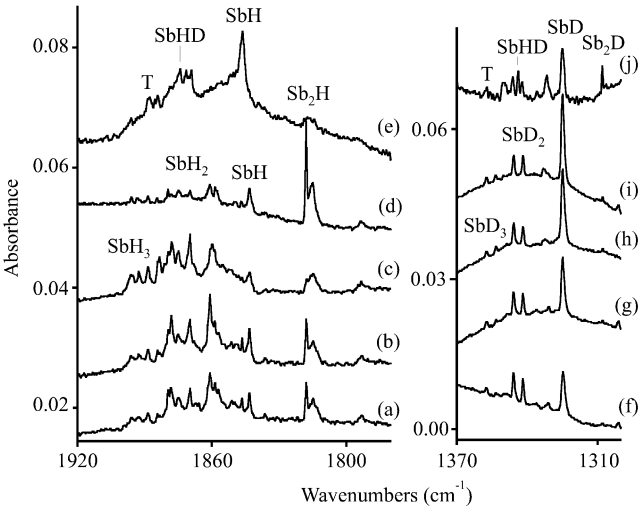

Figure 5. Infrared spectra in the 1920−1780 and 1370−1300 cm^{-1} regions for laser-ablated Sb atoms co-deposited with normal H_2 and D_2 at 3.5 K. (a) Sb and 60 STPcc of H_2 condensed at 3.5 K, (b) after $\lambda > 380$ nm photolysis, (c) $\lambda > 290$ nm photolysis, (d) after annealing to 6.3 K, (e) Sb and 50% H_2 + 50% D_2 after $\lambda > 290$ nm photolysis, (f) Sb and 60 STPcc of D_2 condensed at 3.5 K, (g) after $\lambda > 380$ nm photolysis, (h) $\lambda > 290$ nm photolysis, (i) after annealing to 9 K, and (j) Sb and 50% H_2 + 50% D_2 after $\lambda > 290$ nm photolysis. The label T denotes SbH_xD_y ($x + y = 3$).

Antimony. Infrared spectra of laser-ablated Sb in pure H_2 are complicated, but the spectrum in pure D_2 is relatively straightforward, as illustrated in Figure 5. The absorption bands are given in Table 2. The spectrum of Sb with H_2 + D_2 is dominated by strong 1846.1 and 1324.8 cm^{-1} bands for the monohydride, triplets at 1873.8, 1871.4, 1869.0 cm^{-1} and at 1346.0, 1343.8, 1342.0 cm^{-1} for the dihydride, and weaker bands appear at 1888.3, 1885.1 cm^{-1} and at 1350.5, 1348.9 cm^{-1} for the trihydride. Such a spectrum is shown at the top of Figure 5.

Antimony and H_2 react in excess neon and reveal a strong 1858.2, 1853.8 cm^{-1} doublet (labeled SbH) and weaker features at 1894.4 and 1883.9, 1879.0 cm^{-1} (labeled SbH_3 and SbH_2) (Figure 6). The broad absorption at 1814.6 cm^{-1} increases on final annealing. Deuterium counterparts follow accordingly in the lower region. An experiment with HD gave the same monohydride bands, but slightly shifted dihydride bands, as shown at the top of Figure 6.

TABLE 2: Infrared Absorptions (cm^{-1}) Observed from Co-deposition of Laser-Ablated Sb Atoms and with Ne/H_2, Pure H_2, and Ar/H_2 at 3.5 K

Ne/H_2	Ne/D_2	H_2	D_2	Ar/H_2	Ar/D_2	ident.
		1896		1886.4	1350.4	SbH_3 site
1894.4	1360.8	1892.6	1357.3	1885.0	1350.1	SbH_3
		1888.4	1353.5	1882.4	1349.4	SbH_3 site
		1883				Sb_xH_y
1883.9	1352.0	1878	1345.8	1869.0	1341.8	SbH_2, ν_1 (a_1)
1879.0	1349.4	1869.7	1341.9	1863.7	1337.6	SbH_2 ν_3 (b_2)
		1860	1333			Sb_xH_y
1858.2	1331.8	1846.1	1324.8	1842.0	1320.9	SbH
1853.8	1328.7	1843.2		1838.3	1318.8	SbH site
1814.6	1306.3	1817.9				Sb_2H
		1815.1	1301.3			Sb_2H

The spectra of Sb and H_2 in excess argon are simpler, as argon freezes more rapidly. A strong 1842.0, 1838.3 cm^{-1} doublet (labeled SbH) with an 1846.5 cm^{-1} shoulder and a weaker 1869.0, 1863.7 cm^{-1} doublet with 1866.8, 1861.7 cm^{-1} satellites (labeled SbH_2) are noteworthy (Figure 7). The weak 1882.4 cm^{-1} band is near that assigned previously to SbH_3 in solid argon, using a synthesized SbH_3 sample.[32] Annealing to 11 K to allow diffusion increases both upper features (Figure 7b), but $\lambda > 380$ nm photolysis decreases the SbH_2 doublet and increases the SbH_3 band, which continues with $\lambda > 290$ and $\lambda > 240$ nm irradiation (Figure 7c). A subsequent annealing to 20 K sharpens and increases all features, particularly SbH_2, and a final 25 K annealing increases SbH_2 peaks at the expense of SbH (Figure 7d,e). Analogous spectra were observed for D_2 in excess argon. The HD experiment again gave the same monohydride bands, but the dihydride absorptions formed triplets in both Sb−H and Sb−D stretching regions (Figure 7f).

Calculations. Density functional calculations using pseudopotentials were performed to assist with vibrational assignments of new hydride species. Since BiH is isovalent with NH, a $^3\Sigma^-$ ground state is expected, but Hund's case (c) coupling splits the $^3\Sigma_1^-$ and $^3\Sigma_0^-$ spin components and gives A1 and XO^+ states.[14−19,33] Since the XO^+ state[14] is mostly (76%) $^3\Sigma^-$, it is no surprise that our B3LYP calculations find $^3\Sigma^-$ below $^1\Sigma^-$. Our computed 1853.8 cm^{-1} harmonic frequency is substantially higher than the 1699 cm^{-1} gas-phase value and the 1635.7 cm^{-1} gas-phase fundamental,[10−13] but this systematic error holds throughout our bismuth hydride calculations. Higher level calculations predict a more appropriate 1619 cm^{-1} frequency for BiH.[14]

The BiH_2 radical is predicted to have two observable Bi−H stretching fundamentals about 12 cm^{-1} above BiH. The physically stable BiH_3 molecule is found to have slightly higher frequency fundamentals, but our B3LYP frequencies are 100 cm^{-1} above values computed at a higher level of theory. The latter are in good agreement with gas-phase observations.[3] Attempts to calculate the BiH_4 radical found repulsive structures in C_{2v} and C_{3v} symmetry. The BiH_5 molecule (D_{3h}) is physically stable, but the strong mode is 65 cm^{-1} lower than the BiH fundamental, which is in accord with a previous calculation of weaker bonds.[5] We find BiH_3 to be 14 kcal/mol more stable than BiH + H_2; however, BiH_5 is 80 kcal/mol less stable than BiH_3 + H_2, which is comparable to the 75 kcal/mol value calculated at the RHF level. Hence, BiH_5 cannot be formed in these experiments.

The dibismuth species Bi_2H_2 and Bi_2H_4 are predicted to have high intensity infrared modes with slightly lower frequencies than their monomers.

TABLE 3: Calculated (B3LYP/6-311++G) Structures and Frequencies for Bismuth Hydride Molecules**

molecule	lengths, Å, angles	frequencies, cm^{-1} (intensities, km/mol)
BiH ($^3\Sigma^-$)[a,b]	1.821	1854(318)
BiH ($^1\Sigma^-$)[a,b]	1.818	1869(310)
BiH_2 ($^2B_1$) (C_{2v})	1.816, 90.0°	1867(b_2, 342), 1864(a_1, 280), 778(a_1, 22)
BiH_3 ($^1A_1$) (C_{3v})	1.813, 91.0°	1871(e, 330 × 2), 1868(a_1, 240), 781(e, 12 × 2), 771(a_1, 43)
BiH_5 ($^1A_1'$)[c] (D_{3h})	1.889, 1.815	1820 (a_1', 0), 1789(e′, 270 × 2), 1512 (a_1', 0), 1509 (a_2'', 717), 983 (e″, 0 × 2), 837 (a_2'', 469), 744 (e′, 307 × 2), 422 (e′, 22 × 2)
Bi_2H_2 (^1Ag)[d] (C_{2h})	1.821, 2.808, 90.8°	1851(b_u, 600), 1837(a_g, 0), 598(a_g, 0), 486(a_u, 17), 401(b_u, 18), 166(a_g, 0)
Bi_2H_4 (^1A_g)[e] (C_{2h})	1.817, 3.032, 90.5°, 90.6°	1859(a_u, 575), 1854(b_u, 542), 1845(a_g, 0), 1844(b_g, 0), 776 (b_u, 37), 768(a_g, 0)[f]

[a] BPW91 functional finds a 31 kcal/mol lower $^3\Sigma^-$ state with 1.830 Å bond length, 1820 cm^{-1} frequency, and $^1\Sigma^-$ state with 1.828 Å length and 1834 cm^{-1} frequency. [b] B3LYP functional finds $^3\Sigma^-$ lower by 27 kcal/mol. [c] BiH_5 is 80 kcal/mol higher energy than $BiH_3 + H_2$. [d] Bi_2H_2 is 44 kcal/mol lower energy than 2BiH ($^3\Sigma^-$). [e] Bi_2H_4 is 35 kcal/mol lower energy than $2BiH_2$ ($^2B_1$). [f] Plus six lower real frequencies.

TABLE 4: Calculated (B3LYP/6-311++G) Structures and Frequencies for Antimony Hydride Molecules**

molecule	lengths, Å, angles	frequencies, cm^{-1} (intensities, km/mol)
SbH ($^3\Sigma^-$)	1.721	1952(264)
SbH_2 ($^2B_1$) (C_{2v})	1.715, 90.3°	1981(a_1, 216), 1976(b_2, 265), 876(a_1, 51)
SbH_3 ($^1A_1$) (C_{3v})	1.709, 91.6°	2010(a_1, 156), 2002(e, 246 × 2), 880(e, 22 × 2), 843(a_1, 76)
Sb_2H_2 (^1A_g)[a] (C_{2h})	1.714, 2.687 91.0°	1981(b_u, 441), 1968(a_g, 0), 692(a_g, 0), 545(a_u, 12), 476(b_u, 22), 219(a_g, 0)
Sb_2H_4 (^1A_g)[b] (C_{2h})	1.711, 2.925, 90.6, 91.0	1992(a_u, 419), 1992(b_u, 400), 1987(a_g, 0), 1980(b_g, 0), 874(b_u, 74), 864(a_g, 0)[c]
Sb_2H ($^2A'$) (C_s)	1.719, 2.711, 92.6°	1937(a′, 219), 505(a′, 20), 186(a′, 0)

[a] Sb_2H_2 is 43 kcal/mol lower energy than 2SbH. [b] Sb_2H_4 is 34 kcal/mol lower energy than $2SbH_2$. [c] Plus six lower real frequencies.

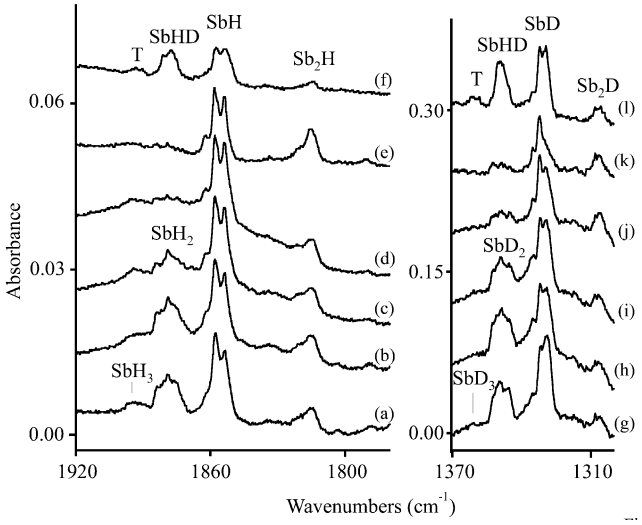

Figure 6. Infrared spectra in the 1920−1780 and 1370−1300 cm^{-1} regions for laser-ablated Sb atoms co-deposited with H_2, D_2, and HD in excess neon at 3.5 K. (a) Sb and 6% H_2 in neon, (b) after annealing to 6.8 K, (c) after $\lambda > 290$ nm photolysis, (d) after $\lambda > 240$ nm photolysis, (e) after annealing to 8 K, (f) Sb and 6% HD in neon, (g) Sb and 6% D_2 in neon, (h) after annealing to 7.5 K, (i) after $\lambda > 380$ nm photolysis, (j) after $\lambda > 240$ nm photolysis, (k) after annealing to 10 K, and (l) Sb and 6% HD in neon. The label T denotes SbH_xD_y ($x + y = 3$).

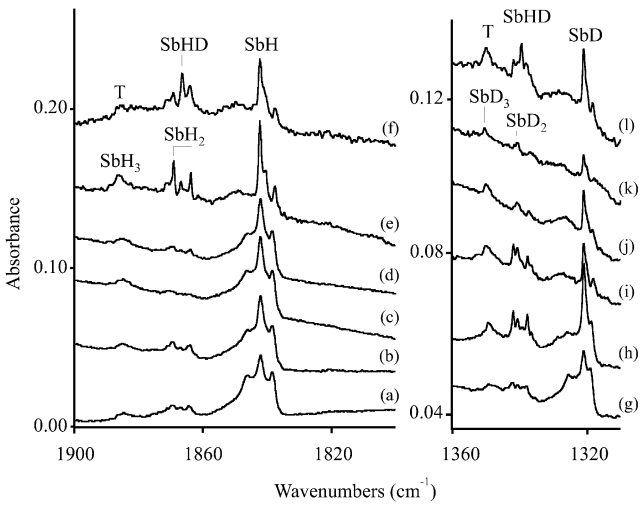

Figure 7. Infrared spectra in the 1920−1780 and 1370−1300 cm^{-1} regions for laser-ablated Sb atoms co-deposited with H_2, D_2, and HD in excess argon at 3.5 K. (a) Sb and 6% H_2 in argon, (b) after annealing to 11 K, (c) after $\lambda > 380$ nm photolysis, (d) after $\lambda > 290$ nm photolysis, (e) after annealing to 25 K, (f) Sb and 6% HD in argon, spectrum after deposition, annealing, photolysis, and annealing to 25 K, (g) Sb and 6% D_2 in argon, (h) after annealing to 19 K, (i) after annealing to 25 K, (j) after $\lambda > 240$ nm photolysis, (k) after annealing to 30 K, and (l) Sb and 6% HD in argon, spectrum after deposition, annealing, photolysis, and annealing to 25 K. The label T denotes SbH_xD_y ($x + y = 3$).

Our calculation for $^3\Sigma^-$ ground-state SbH finds a 1952 cm^{-1} harmonic frequency, which is slightly higher than the experimental value (ω_e, 1923 cm^{-1}; ν_o, 1855 cm^{-1})[34] and in accord with a recent 1886 cm^{-1} ab initio value.[35] We predict the SbH_2 radical to have observable modes 24−29 cm^{-1} higher than those of SbH. The stable SbH_3 molecule[1,32,36] is predicted to absorb 50−58 cm^{-1} higher than SbH, which is in agreement with earlier frequency calculations.[7]

Analogous B3LYP calculations predict stable diantimony species Sb_2H_2 and Sb_2H_4 with absorptions above their monomers and Sb_2H with strong absorption below SbH.

Discussion

The metal hydride product absorptions will be assigned on the basis of isotopic shifts, matrix shifts, comparison to trends in calculated frequencies, and known vibrational spectra.

Monohydrides. The strongest product absorption in each laser-ablated metal and hydrogen system is the monohydride diatomic molecule SbH or BiH. First, the SbH bands at 1858.2, 1846.1, and 1842.0 cm^{-1} in solid neon, hydrogen, and argon, respectively, exhibit 1.395, 1.394, and 1.394 SbH/SbD frequency ratios, which are nearly the same as the 1.393 ratio observed for the 1854.8 cm^{-1} gas-phase fundamental vibration.[34] Second, the SbH and SbD bands are invariant when $H_2 + D_2$ or HD is used as the reagent gas, hence one H(D) atom is involved in the vibration.

The BiH absorptions at 1635.9, 1622.7, and 1621.9 cm^{-1} in solid neon, hydrogen, and argon, respectively, exhibit 1.395, 1.395, and 1.396 BiH/BiD ratios, which are almost identical to the 1.394 ratio found for the gas-phase 1635.7 cm^{-1} vibrational fundamental.[10−13] Again, note that the neon matrix value is slightly higher and the hydrogen and argon matrix values are slightly lower than the gas-phase observation. Although the BiH and BiD bands are invariant with the $H_2 + D_2$, and HD reagents in neon and argon matrixes, and BiD is invariant in D_2 and $H_2 + D_2$ samples, the BiH bands are perturbed by the solid normal hydrogen (ortho and para)[37] matrix environment. The BiH band is 1623.3 cm^{-1} with $H_2 + D_2$ mixtures and split 1628.8, 1627.1, 1624.0 cm^{-1} in pure HD. On annealing to 6.1 K, the 1622.7 and 1630.0 cm^{-1} features give way to a sharp 1633.3 cm^{-1} absorption (Figure 1b); however, ultraviolet photolysis restores and increases the 1630.0 and 1622.7 cm^{-1} bands (Figure 1c,d), and a subsequent 6.6 K annealing restores the sharp 1633.3 cm^{-1} feature (Figure 1e). The 1163.4 cm^{-1} BiD band in normal solid deuterium is little affected by similar operations (Figure 1f−j). The central difference between solid normal hydrogen and deuterium is that 3/4 of the H_2 molecules are in the $J = 1$ state (ortho) with 354 cm^{-1} of rotational energy, but only 1/3 of the D_2 molecules are in the $J = 1$ state (para) with 179 cm^{-1} of rotational energy.[37] Hence the largely $^3\Sigma^-$ ground-state BiH molecule is sustaining more perturbation from the solid hydrogen matrix than BiD in solid deuterium. This is true to a lesser extent for SbH, where the major absorption at 1843.2 cm^{-1} in solid hydrogen gives way to a strong 1846.1 cm^{-1} band in mixed $H_2 + D_2$ (Figure 5e,f).

The BiH molecules are produced here in the endothermic reaction 1 that is activated by excess electronic/kinetic energy[25,26] in the laser-ablated Bi atoms. This reaction occurs inside a heat pipe oven for the gas-phase measurements.[10] The reaction energies are estimated by B3LYP/SDD computations.

$$Bi + H_2 \rightarrow BiH + H \quad [\Delta E = 47 \text{ kcal/mol}] \qquad (1)$$

Dihydrides. The sharp doublet at 1869.0 and 1863.7 cm^{-1} with Sb and H_2 in solid argon shifts to 1341.8 and 1337.6 cm^{-1} with deuterium substitution. These bands exhibit 1.3929 and 1.3933 H/D frequency ratios. Single intermediate 1866.5 and 1339.6 cm^{-1} bands were dominant with the HD reagent (Figure 7f). Note that these intermediate features are within experimental accuracy (±0.1 cm^{-1}) of the average doublet component frequency. This points to the (symmetric and antisymmetric) vibrations of two equivalent hydrogen atoms using H_2 and the single intermediate feature is due to the single H(D) vibration in each region. The neon matrix samples gave a slightly resolved version of the argon matrix spectrum at slightly higher frequencies, and HD substitution produced an intermediate peak. Although the deuterium matrix exhibited a sharp 1345.8 and 1341.9 cm^{-1} doublet, the hydrogen matrix spectrum is again complicated by matrix interaction, but the sharp 1869.7 cm^{-1} bands appears to be due to this species. However, pure $H_2 + D_2$ again gave triplet patterns, at 1873.8, 1871.4, and 1869.0 cm^{-1} and at 1346.0, 1343.8, and 1342.0 cm^{-1}, where the central intermediate component is again a result of the mixed isotopic molecule. The above isotopic patterns identify the SbH_2 molecule from two (a_1 and b_2) stretching vibrations.

This assignment to SbH_2 is supported by B3LYP calculations, which predict two observable stretching modes above SbH by 24−29 cm^{-1}, in agreement with the 22−27 cm^{-1} displacements observed.

In a former investigation with SbH_3 (SbD_3) in solid argon, full-arc photolysis produced weak new 1840.5 (1320.2) cm^{-1} bands.[32] Since an early RECP calculation[38] predicted SbH absorption much lower at 1763 cm^{-1}, the 1840.5 cm^{-1} absorption was assigned to the SbH_2 radical in solid argon. The present work shows that the weak photolysis product bands are due to SbH(SbD), in accord with flash photolysis of SbH_3 in the gas phase.[39]

The strongest sharp bands at 1699.1 and 1692.7 cm^{-1} with Bi in pure hydrogen after $\lambda > 240$ nm photolysis exhibit the same behavior and are a result of BiH_2. First, the shift to 1218.4 and 1214.4 cm^{-1} in pure deuterium provides H/D frequency ratios 1.3945 and 1.3938, which are appropriate for BiH(D) vibrations. Second, the $H_2 + D_2$ and HD experiments produce triplet bands with intermediate components for the BiHD molecule. These triplets change relative intensities with $H_2 + D_2$ composition for the three molecules BiH_2, BiHD, and BiD_2 formed; with pure HD the central BiHD components clearly dominate. Similar partially resolved bands are observed for neon samples, but the bands are sharp in solid argon and three bands are again observed in each region with H_2, D_2, and HD samples (Figure 4). These three bands, two for antisymmetric and symmetric Bi−H_2 modes and one intermediate peak for Bi−H in BiHD, confirm the identification of a dihydride. The BiH_2 bands are slightly higher in solid neon and slightly lower in solid argon (with the same 6.4−6.9 cm^{-1} b_2−a_1 mode separation), which is the same trend observed for SbH_2, SnH_2, and PbH_2.[40] The weaker satellites at 1708.4 and 1701.5 cm^{-1} in solid hydrogen are believed to be a result of different matrix interactions (sites).

This assignment is supported by B3LYP calculations, which predict two separate modes slightly higher than BiH, but the agreement is not as good as found for SbH_2. This work reports the first experimental evidence for the SbH_2 and BiH_2 radicals.

The BiH_2 radical can be formed by two routes: the H atom reaction 2 or the H_2 reaction 3. Hydrogen atoms are a byproduct of reaction 1 and impact with laser-ablated Bi atoms or photons from the emission plume.[25,26] It appears that reaction 3 is promoted by $\lambda > 240$ nm photolysis in these experiments. Even though reaction 3 appears to be exothermic, the growth of BiH_2 on annealing in solid argon is most likely a result of reaction 2.

$$BiH\ (^3\Sigma^-) + H \rightarrow BiH_2\ (^2B_1) \quad [\Delta E = -58 \text{ kcal/mol, B3LYP}] \qquad (2)$$

$$Bi\ (^4S) + H_2\ (^1\Sigma g^+) \rightarrow BiH_2\ (^2B_1) \quad [\Delta E = -11 \text{ kcal/mol}] \qquad (3)$$

Trihydrides. The weak 1885.0 and 1350.1 cm^{-1} bands with Sb and H_2, and Sb and D_2 in excess argon are near very strong 1882.2 and 1352.7 cm^{-1} absorptions measured with the authentic material.[32] These bands shift slightly to 1894.4 and 1360.8 cm^{-1}

in excess neon, near the 1894 and 1362 cm^{-1} gas-phase values.[36] In pure hydrogen and pure deuterium, split bands are observed near 1892.6 and 1357.3 cm^{-1}, respectively. These weak absorptions are clearly a result of $SbH_3(SbD_3)$, which is formed here by H atom reactions with SbH and SbH_2.

The weak 1726.2 cm^{-1} absorption with Bi in pure hydrogen is destroyed by $\lambda > 240$ nm photolysis, but it is restored in part on 6.6 K annealing. This band shifts to 1239.0 cm^{-1} in pure deuterium, which gives a 1.393 ratio. Corresponding weak bands are observed at 1726.0 and 1238.5 cm^{-1} in $H_2 + D_2$ and at 1727.7 and 1239.7 cm^{-1} in pure HD. Our B3LYP calculations predict less than a 1 cm^{-1} shift for the strongest modes of BiH_2D and $BiHD_2$ relative to BiH_3 and BiD_3. Hence, the weak 1726.2 and 1239.0 cm^{-1} bands are assigned to the ν_3(e) modes of BiH_3 and BiD_3, and the weak bands in pure HD are a result of BiH_2D and $BiHD_2$. Neon matrix experiments reveal weak 1733.6 and 1243.3 cm^{-1} absorptions for BiH_3 and BiD_3.

The BiH_3 molecule was observed by high-resolution IR spectroscopy one year ago,[3] and the ν_3(e) fundamental was measured at 1734.5 cm^{-1}. Our 1726.2 cm^{-1} hydrogen matrix and 1733.6 cm^{-1} neon matrix bands are in excellent agreement; in addition we observe BiD_3 in solid deuterium. Even though BiH_3 is a molecule of limited gas-phase stability,[3] BiH_3 is synthesized by the H atom and H_2 molecule reactions 4 and 5. We suspect that reaction 5 has activation energy and that reaction 4 is the preferred route.

$$BiH_2 + H \rightarrow BiH_3\,(^1A_1) \quad [\Delta E = -60\ \text{kcal/mol}] \quad (4)$$

$$H_2 + BiH\,(^3\Sigma^-) \rightarrow BiH_3\,(^1A_1) \quad [\Delta E = -14\ \text{kcal/mol}] \quad (5)$$

$$BiH_3 + H_2 \rightarrow BiH_5 \quad [\Delta E = 80\ \text{kcal/mol}] \quad (6)$$

Finally, we find no evidence of absorption in the region below BiH calculated here for BiH_5, which is in accord with its thermochemical instability.[5,6] Although BiH_3 has just been characterized,[3] this is the first observation of BiD_3.

Polymetal Hydrides. The 1815.1 cm^{-1} band with hydrogen and 1301.3 cm^{-1} deuterium counterpart remain after final annealing in experiments with Sb. The 1.395 H/D frequency ratio is appropriate for an Sb−H(D) vibration, and the appearance 31(23) cm^{-1} below SbH(D) is in accord with calculations for $Sb_2H(D)$, which find strong absorptions 15(11) cm^{-1} lower. Accordingly, the 1815.1 cm^{-1} band is assigned to Sb_2H.

B3LYP calculations for Sb_2H_2 and Sb_2H_4 predict strong absorptions 29 and 40 cm^{-1} above SbH. This region contains extra absorptions that are probably due to such higher metal hydride clusters.

A real possibility exists that one of the bands 12 cm^{-1} below BiH could be due to Bi_2H_2, but neither observations nor calculations are of sufficient quality to justify a definitive assignment. It is also possible that similar Bi_xH_y clusters are observed in the 1680−1650 cm^{-1} region, although calculated frequencies do not fit observed bands as well.

Conclusions

Laser-ablated Sb and Bi atoms react with hydrogen during condensation in excess hydrogen, neon, and argon to form the SbH and BiH diatomic molecules. The SbH_2 and BiH_2 radicals are observed here for the first time. In addition, the SbH_3 and BiH_3 trihydrides are produced. Although BiH_3 is of limited stability in the gas phase, BiH_3 is formed by further H atom reactions with BiH_2 in solid hydrogen and neon. No evidence is found for the thermochemically unstable BiH_5 molecule.

Acknowledgment. We thank NSF for financial support under Grant CHE00-78836.

References and Notes

(1) Cotton, F. A.; Wilkinson, G.; Murillo, C. A.; Bochmann, M. *Advanced Inorganic Chemistry*, 6th ed.; Wiley: New York, 1999.
(2) Amberger, E. *Chem. Ber.* **1961**, *94*, 1447.
(3) Jerzembeck, W.; Bürger, H.; Constantin, L.; Margulès, L.; Demaison, J.; Breidung, J.; Thiel, W. *Angew. Chem., Int. Ed.* **2002**, *41*, 2550.
(4) Dai, D.; Balasubramanian, K. *J. Chem. Phys.* **1990**, *93*, 1837.
(5) Schwerdtfeger, P.; Heath, G. A.; Dolg, M.; Bennett, M. A. *J. Am. Chem. Soc.* **1992**, *114*, 7518.
(6) Schwerdtfeger, P.; Laakkonen, J.; Pyykkö, P. *J. Chem. Phys.* **1992**, *96*, 6807.
(7) Breidung, J.; Thiel, W. *J. Mol. Spectrosc.* **1995**, *169*, 166.
(8) Gomez, S. S.; Romero, R. H.; Aucar, G. A. *J. Chem. Phys.* **2002**, *117*, 7942.
(9) Moc, J.; Morokuma, K. *J. Am. Chem. Soc.* **1995**, *52*, 393.
(10) Bopegedera, A. M. R. P.; Brazier, C. R.; Bernath, P. F. *Chem. Phys. Lett.* **1989**, *162*, 301.
(11) Fink, E. H.; Setzer, K. D.; Ramsay, D. A.; Vervloet, M.; Brown, J. M. *J. Mol. Spectrosc.* **1990**, *142*, 108.
(12) Urban, R.-D.; Polomsky, P.; Jones, H. *Chem. Phys. Lett.* **1991**, *181*, 485.
(13) Hedderich, H. G.; Bernath, P. F. *J. Mol. Spectrosc.* **1993**, *158*, 170.
(14) Balasubramanian, K. *Chem. Phys. Lett.* **1985**, *114*, 201. *J. Mol. Spectrosc.* **1986**, *115*, 258.
(15) Ramos, A. F.; Pyper, N. C.; Malli, G. L. *Phys. Rev. A* **1988**, *38*, 2729.
(16) Dai, D.; Balasubramanian, K. *J. Chem. Phys.* **1990**, *93*, 1837.
(17) Dolg, M.; Kuchle, W.; Stoll, H.; Preuss, H.; Schwerdtfeger, P. *Mol. Phys.* **1991**, *74*, 1265.
(18) Alekseyev, A. B.; Buenker, R. J.; Liebermann, H.-P.; Hirsch, G. *J. Chem. Phys.* **1994**, *100*, 2989.
(19) Wildman, S. A.; Dilabio, G. A.; Christiansen, P. A. *J. Chem. Phys.* **1997**, *107*, 9975.
(20) Han, Y.-K.; Bae, C.; Lee, Y. S.; Lee, S. Y. *J. Comput. Chem.* **1998**, *19*, 1526.
(21) Wang, X.; Andrews, L. *J. Phys. Chem. A* **2003**, *107*, 570 (Cr + H_2).
(22) Wang, X.; Andrews, L. *J. Am. Chem. Soc.* **2003**, *125*, 6581 (PbH_4).
(23) Weltner, W., Jr.; Van Zee, R. J.; Li, S. *J. Phys. Chem.* **1995**, *99*, 6277.
(24) Tam, S.; Macler, M.; DeRose, M. E.; Fajardo, M. E. *J. Chem. Phys.* **2000**, *113*, 9067.
(25) Burkholder, T. R.; Andrews, L. *J. Chem. Phys.* **1991**, *95*, 8697.
(26) Andrews, L.; Citra, A. *Chem. Rev.* **2002**, *102*, 885.
(27) Frisch, M. J.; Trucks, G. W.; Schlegel, H. B.; Scuseria, G. E.; Robb, M. A.; Cheeseman, J. R.; Zakrzewski, V. G.; Montgomery, J. A., Jr.; Stratmann, R. E.; Burant, J. C.; Dapprich, S.; Millam, J. M.; Daniels, A. D.; Kudin, K. N.; Strain, M. C.; Farkas, O.; Tomasi, J.; Barone, V.; Cossi, M.; Cammi, R.; Mennucci, B.; Pomelli, C.; Adamo, C.; Clifford, S.; Ochterski, J.; Petersson, G. A.; Ayala, P. Y.; Cui, Q.; Morokuma, K.; Malick, D. K.; Rabuck, A. D.; Raghavachari, K.; Foresman, J. B.; Cioslowski, J.; Ortiz, J. V.; Stefanov, B. B.; Liu, G.; Liashenko, A.; Piskorz, P.; Komaromi, I.; Gomperts, R.; Martin, R. L.; Fox, D. J.; Keith, T.; Al-Laham, M. A.; Peng, C. Y.; Nanayakkara, A.; Gonzalez, C.; Challacombe, M.; Gill, P. M. W.; Johnson, B.; Chen, W.; Wong, M. W.; Andres, J. L.; Gonzalez, C.; Head-Gordon, M.; Replogle, E. S.; Pople, J. A. *Gaussian 98*, Revision A.6; Gaussian, Inc.: Pittsburgh, PA, 1998.
(28) (a) Becke, A. D. *Phys. Rev. A* **1988**, *38*, 3098. (b) Perdew, J. P.; Wang, Y. *Phys. Rev. B* **1992**, *45*, 13244.
(29) (a) Becke, A. D. *J. Chem. Phys.* **1993**, *98*, 5648. (b) Lee, C.; Yang, E.; Parr, R. G. *Phys. Rev. B* **1988**, *37*, 785.
(30) (a) Krishnan, R.; Binkley, J. S.; Seeger, R.; Pople, J. A. *J. Chem. Phys.* **1980**, *72*, 650. (b) Frisch, M. J.; Pople, J. A.; Binkley, J. S. *J. Chem. Phys.* **1984**, *80*, 3265.
(31) Andrae, D.; Haussermann, U.; Dolg, M.; Stoll, H.; Preuss, H. *Theor. Chim. Acta* **1990**, *77*, 123.
(32) Andrews, L.; Moores, B. W.; Fonda, K. K. *Inorg. Chem.* **1989**, *28*, 290.
(33) Lindgren, B.; Nilsson, Ch. *J. Mol. Spectrosc.* **1975**, *55*, 407.
(34) Urban, R.-D.; Essig, K.; Jones, H. *J. Chem. Phys.* **1993**, *99*, 1591.
(35) Alekseyev, A. B.; Liebermann, H.-P.; Lingott, R. M.; Bludsky, O.; Buenker, R. J. *J. Chem. Phys.* **1998**, *108*, 7695.
(36) Haynie, W. H.; Nielsen, H. H. *J. Chem. Phys.* **1953**, *21*, 1838.
(37) Silvera, I. F. *Rev. Mod. Phys.* **1980**, *52*, 393.
(38) Balasubramanian, K.; Tanpipat, N.; Bloor, J. E. *J. Mol. Spectrosc.* **1987**, *124*, 458.
(39) Bollmark, P.; Lindgren, B. *Chem. Phys. Lett.* **1967**, *1*, 480.
(40) Wang, X.; Andrews, L.; Chertihin, G. V.; Souter, P. F. *J. Phys. Chem. A* **2002**, *106*, 6302.